

Effects of algebraic singularities on the voltage dynamics of differential-algebraic power system model

Saffet Ayasun^{*,†}

Department of Electrical and Electronics Engineering, Nigde University, 51100, Nigde, Turkey

SUMMARY

Voltage stability analysis of differential-algebraic equation (DAE) power system model is more complicated than for systems described by ordinary differential equations (ODEs). In addition to unstable equilibria, algebraic singularity plays a crucial role in assessing the voltage stability. This paper explores the algebraic structure and singularities of the DAE model to investigate its influence on the voltage stability. Singular points are identified at various load levels and are illustrated together with the equilibria using nose curves. Then, at a given load level, the constraint manifold is decomposed into the voltage casual regions and singular points connecting them. Time-domain simulations initiated in the vicinity of singular points are performed to determine how singular points affect system dynamics. It is shown that depending on the relative location of initial points with respect to singular points, trajectories of bus voltages may settle to an infeasible low voltage stable equilibrium point, which may cause a further disturbance in the system leading a voltage stability problem. Copyright © 2007 John Wiley & Sons, Ltd.

KEY WORDS: differential-algebraic equation model; voltage stability; constraint manifold; singular point; singularity induced bifurcation

1. INTRODUCTION

The differential-algebraic equations (DAEs) are widely used to investigate various types of stability problems in electrical power systems [1]. These stability problems include voltage stability and collapse [2–5], oscillatory instabilities [6,7] and local bifurcations of equilibria and associated stability problems such as small-signal stability [8–15]. This paper investigates the effect of the algebraic singularities on the dynamic of a classical power system with constant PQ load buses, which is modeled as semi-explicit index-1 DAEs of the form [2,9]:

$$\begin{aligned}\dot{x} &= f(x, y, \beta) \\ 0 &= g(x, y, \beta)\end{aligned}\tag{1}$$

*Correspondence to: Saffet Ayasun, Department of Electrical and Electronics Engineering, Nigde University, 51100, Nigde, Turkey.

†E-mails: sayasun@nigde.edu.tr; saffet@nwankpa.ece.drexel.edu; saffetayasun@yahoo.com

The DAE model of (1) has two essential features: (1) explicit parameter dependence; (2) differential-algebraic structure. The parameter dependence implies that the system equilibria may exhibit local bifurcations when parameters are subject to variation. These bifurcations are saddle node (SN), Hopf and singularity induced (SI) bifurcations. The SN and Hopf bifurcations, which are also observed in ODE models of power systems, have been extensively studied in power systems and they are linked to voltage collapse and oscillatory instabilities, respectively [9]. The SI bifurcation is due to singularity of the algebraic equations of the DAE model under some parameter variations. The SI bifurcation occurs when system equilibria encounter the singularity manifold and it refers to a stability change owing to one or two of the eigenvalues of the reduced Jacobian matrix associated with the equilibrium diverging to infinity [10]. Several recent papers report on the existence of SI bifurcations in various size power systems including a real power system (South Brazilian power system) [12] and the standard IEEE test systems [13,14].

The differential-algebraic structure plays a crucial role in investigating the dynamics of power systems. The algebraic equation requires that trajectories of DAE systems be restricted to a set known as the constraint manifold. The constraint manifold is defined as a set of points that satisfy the algebraic part of Equation (1). The general methods for studying the power system dynamics require the reduction of the DAE model to a locally equivalent set of ODEs. Typically, in a major part of the constraint manifold such a reduction is possible and the ODEs uniquely define the dynamic behavior of DAEs. Points at which the reduction can be achieved are referred to as causal points [2]. The constraint manifold will in general contain singular points at which equivalence is not possible. Singular points are points on the constraint manifold at which the algebraic Jacobian matrix is singular and thus, the vector field is not well defined. In terms of power system dynamics, around singular points load bus variables (algebraic variables) cannot be defined in terms of the generator angles (the natural state variables). Thus, the causal requirement of the DAE model breaks down and it cannot predict system behavior. In power systems such points were encountered by DeMarco and Bergen [16] in connection with transient stability studies (impasse points), and by Kwatny *et al.* [2] in connection with static bifurcation analysis (noncausal points). Hiskens and Hill [17,18] have extended the concept of voltage causal points to a voltage causal region within which load bus variables closely follow the generator angle behavior and the DAE model could be reduced to a set of ODEs. The constraint manifold was decomposed into voltage causal regions separated by the singular surface (impasse surface). Their studies reveal the fact that there is a relationship between voltage instability and loss of voltage causality. Especially, trajectories passing near a singular point may bifurcate and the voltage magnitudes may settle to a physically infeasible operating point (i.e., low voltage profile). In Reference [4], Praprost and Loparo have reported similar results, and using the bifurcation theory they have shown that an important part of the stability boundary is formed by trajectories that are tangent to the singular surface (boundary of solution sheets). Therefore, these studies indicate that location of singularities, which constitute important organizing elements of a power system DAE model, is invaluable information for assessing stability of the system.

We have recently [13,19] presented an iterative method to identify algebraic singularities including the SI bifurcation of the DAE model of power systems. In the method, generator angles were used to parameterize the algebraic part of the DAE model at any given parameter value (i.e., bus injections) and singular points were computed as being the SN bifurcation of algebraic part of the DAE model. Using two-dimensional (2-D) PV curves (nose curves) singular points were depicted together with the equilibria and their associated local bifurcations as a function of the parameters to give a visual representation of both static and dynamic stability boundaries in the same picture. This work extends our earlier work reported in References [13] and [19]. The aim of this paper is to analyze power system

dynamics around singular points and especially to show how location of singular points affects the voltage trajectories of the system using time-domain simulations. The analysis presented in this paper involves the following three main steps:

1. Computing singular points at various parameter values along the nose curve defined by a designated load increase pattern and illustrating them in the nose curve together with the equilibrium points [13];
2. Decomposition of the constraint manifold into voltage causal regions separated by singular points at a given parameter value;
3. Investigating angle and voltage trajectories initiated at points arbitrarily close to singular points located on the boundary segment of voltage causal regions.

Using a 5-bus power system, it is shown that each voltage causal region contains only a stable equilibrium point and singular points lie on the boundary of the stability region (region of attraction) of the corresponding equilibrium point. Time-domain simulations indicate that trajectories initiated at points, each of which are located in a different voltage region and arbitrarily close to a singular point, reach the stable equilibrium point in that region. However, some of these equilibrium points, though stable, may not be a feasible operating point due to their low voltage profiles, which may cause a further disturbance in the system leading a voltage stability problem. It is also shown that angle deviations among stable equilibrium points are not significant, which may lead to erroneous conclusions about feasible states.

2. SINGULARITIES AND DYNAMICS OF DAE POWER SYSTEM MODEL

For dynamic stability analysis of power system, equilibrium points (operating points) at a given set of parameters and their small-signal stability features are first needed to be determined. For a given set of parameters β , an equilibrium point must satisfy two sets of algebraic equations of DAE model of (1). The set of all equilibrium points is defined as follows:

$$E = \{(x, y, \beta) \in \mathfrak{R}^{n+m+k} | f(x, y, \beta) = 0, g(x, y, \beta) = 0\} \quad (2)$$

The small-signal stability features of an equilibrium point, say (x_0, y_0) , are characterized by the eigenvalues of the reduced (linearized) system matrix if $[D_y g(x, y, \beta)]$ is nonsingular.

$$[A_{\text{sys}}] = [D_x f]|_0 - [D_y f]|_0 [D_y g]|_0^{-1} [D_x g]|_0 \quad (3)$$

For an equilibrium point to be small-signal stable, all eigenvalues of the reduced system matrix must lie on the left half part of the complex plane. The stability of an equilibrium point could be easily verified by integrating the DAE model of (1) with an initial condition given around the corresponding equilibrium point. The stability of the DAE systems is more complicated than for systems described by ODEs due to the algebraic structure of the model. The algebraic part of Equation (1) requires that any motion be constrained to the manifold:

$$M(\beta) = \{(x, y) \in \mathfrak{R}^{n+m} | g(x, y, \beta) = 0, \beta = \text{constant}\} \quad (4)$$

The manifold M is the *state space* for the dynamical system defined by Equation (1) which induces a vector field on M . The vector field may not be well defined at all points of M . At any point $(x, y) \in M$ we have $\dot{x} = f(x, y, \beta)$, and if $[D_y g(x, y, \beta)]$ is nonsingular, then \dot{y} is uniquely defined by

$$\dot{y} = - \left[\frac{\partial g}{\partial y} \right]^{-1} \left[\frac{\partial g}{\partial x} \right] [f(x, y, \beta)] \quad (5)$$

If $[D_y g(x, y, \beta)]$ is singular at a point $(x, y) \in M$ then vector field is not well defined at that point. Typically, such singular points lie on codimension 1 submanifolds of M .

Definition [2]: Suppose M is a regular manifold for all β near β^* , and that $\det[D_y g(x, y)] \neq 0$ at a point $\beta = \beta^*$, $(x, y) = (x^*, y^*) \in M$. Then (x^*, y^*, β^*) is said to be causal. Otherwise it is noncausal. ■

The causality of a point could be extended to the causality of a region as follows [17,18]:

$$C_p(\beta) = \left\{ (x, y) \in M \mid \det[D_y g(x, y, \beta)] \neq 0; \right. \\ \left. [D_y g(x, y, \beta)]|_{(x,y)} \text{ has } p \text{ negative real eigenvalues} \right\} \quad (6)$$

Within any voltage causal region load bus voltages and angles follow generator angles' behavior. At any causal point (x^*, y^*, β^*) in the region, the implicit function theorem ensures that there exists a function $\psi_p(x, \beta)$ defined on a neighborhood of (x^*, β^*) with $y^* = \psi_p(x^*, \beta^*)$ and that satisfies $g(x, \psi_p(x, \beta), \beta) = 0$. It follows that within a voltage causal region, trajectories of the DAE are locally defined by the ODEs:

$$\dot{x} = \phi_p(x, \beta) = f(x, \psi_p(x, \beta), \beta) \quad (7)$$

Typically, in a major part of the constraint manifold such a reduction is possible and the ODEs uniquely define the dynamics of DAEs. However, the constraint manifold will in general contain noncausal points (or singular points) at which equivalence is not possible. These singular points that lie in the boundary of voltage causal regions form a singular surface (or impasse surface) in the constraint manifold [3,18]:

$$S(\beta) = \left\{ (x, y) \in \mathfrak{R}^{n+m} \mid g(x, y, \beta) = 0, \det[D_y g(x, y, \beta)] = 0 \right\} \quad (8)$$

Over casual regions, system dynamic behavior evolves according to a locally equivalent ODE system representation. However, trajectories that encounter the singular surface typically undergo loss of existence/uniqueness. The singularity of $[D_y g(x, y, \beta)]$ (similarly, unbounded eigenvalue of $[A_{\text{sys}}]$) implies that the system will experience some sort of instability problem resulting from fast interactions of network variables. However, it is difficult to predict the nature of instability owing to modeling limitations. The DAE model cannot predict the system behavior and the validity of the model, as a characterization of the power system, is questionable. It is likely that uncertainties, neglected in the DAE model, now become central to the local behavior of the system. Praprost and Loparo [4] (much earlier DeMarco and Bergen [16]) have proposed a singularly perturbed differential equation (SPDE) as the power system model to avoid the singularities, and their simulation results indicate that rapid decline in bus voltage magnitudes may occur if trajectories pass close to the singular surface.

It has been observed in power systems that for certain parameter value $\beta = \beta_{\text{SI}}$ an equilibrium point, say (x_0, y_0) may be located at the singularity of the algebraic equation $g(x, y, \beta) = 0$, which is known as the SI bifurcation. The SI bifurcation refers to stability change due to an eigenvalue of the reduced system matrix associated with the equilibrium point diverging to infinity from either $-\infty$ to $+\infty$, or

vice versa without crossing the $j\omega$ -axis [3,10]. The set of SI bifurcations is defined as follows:

$$SI(\beta) = \left\{ (x, y, \beta) \in \mathfrak{R}^{n+m+k} \mid \begin{array}{l} f(x, y, \beta) = 0, g(x, y, \beta) = 0 \\ \det[D_y g(x, y, \beta)] = 0 \end{array} \right\} \quad (9)$$

In the DAE model of classical power systems with constant PQ load buses, the differential equations represent the swing equations of generators and algebraic equations are the power flow equations representing real and reactive power balances at the PQ load buses. For a network consisting of the n_g number of generators and n_{pq} number of PQ load buses, the number of differential and algebraic equations are $2(n_g - 1)$ and $2n_{pq}$, respectively. It must be mentioned that the generator bus #1 is generally chosen as the swing bus of the system (i.e., voltage magnitude and angle are assumed to be known for this bus) and all other phase angles are measured relative to the swing bus. For this reason, differential equations include the swing equations (two equations for each generator) of the rest of $(n_g - 1)$ number of generators [2]. The vector of dynamic state variables $x = [\delta_g \ \omega]^T$ represents the rotor angles and angular velocities of the $(n_g - 1)$ number of generators and thus its length is $2(n_g - 1)$. The vector of algebraic state variables $y = [\delta_\ell \ V]^T$ represents phase angles and magnitudes of voltages at the n_{pq} number of PQ load buses and thus its length is $2n_{pq}$. The set of parameter $\beta = [\beta_g \ \beta_\ell]^T$ represents real/reactive power injections at the buses and β_g parameter vector is in the form of $\beta_g = [0^T \ (-M^{-1} P_g)^T]^T$ where $P_g = [P_2 \ \dots \ P_{n_g}]^T$ denotes net real power injections to the $(n_g - 1)$ number of generators and M is the inertia matrix. Therefore, the length of β_g is $2(n_g - 1)$. The set of parameters $\beta_\ell = [P_\ell^T \ Q_\ell^T]^T$ denotes the load demands at the n_{pq} number of load buses where $P_\ell = [P_{n_g+1} \ \dots \ P_{n_g+n_{pq}}]^T$ and $Q_\ell = [Q_{n_g+1} \ \dots \ Q_{n_g+n_{pq}}]^T$ are the real and reactive power demands, respectively. The length of β_ℓ is $2n_{pq}$. Finally, it is evident that the length of parameter vector β is $2(n_g - 1) + 2n_{pq}$. For the sake of simplicity in the notation, in the previous discussion on the dynamics of DAE power systems, it is assumed that $x \in \mathfrak{R}^n$, $y \in \mathfrak{R}^m$, and $\beta \in \mathfrak{R}^k$ where $n = 2(n_g - 1)$, $m = 2n_{pq}$, and $k = 2(n_g - 1) + 2n_{pq}$.

Local bifurcation analyses of power systems identify qualitative changes in system equilibria, such as number of equilibria and their small-signal stability features as the bus injections are subject to vary. Changes in bus injections are achieved through parameterization of bus injections with a scalar parameter known as a bifurcation parameter.

$$\beta = \beta^0 + \alpha^* \text{direction } \beta \quad (10)$$

where β^0 is the base case bus injections, α is the scalar bifurcation parameter and $\text{direction}\beta = [d_{P_g}^T \ d_{P_\ell}^T \ d_{Q_\ell}^T]^T$ is the direction vector in the parameter space, which allows us to vary bus injections at a single bus and/or a group of buses. The elements of $\text{direction } \beta$ are given below:

$$d_{P_g} = [d_{P_2} \ \dots \ d_{P_{n_g}}]^T; \ d_{P_\ell} = [d_{P_{n_g+1}} \ \dots \ d_{P_{n_g+n_{pq}}}]^T; \ d_{Q_\ell} = [d_{Q_{n_g+1}} \ \dots \ d_{Q_{n_g+n_{pq}}}]^T \quad (11)$$

The elements of d_{P_g} , d_{P_ℓ} , and d_{Q_ℓ} can be set to be positive, negative, or zero depending on the load increase scenario of interest. For example, if one wants to increase real power injections into some selected generator buses, then the corresponding elements of d_{P_g} are set to be positive. Similarly, in order to increase real/reactive power demand at some selected buses, one needs to set the corresponding entries of d_{P_ℓ} and d_{Q_ℓ} to be negative.

The evolution of system equilibria and their small-signal stability features as the bifurcation parameter α varies are usually illustrated through the two-dimensional (2-D) equilibrium surfaces known as nose or PV curves. Figure 1 schematically shows such a nose curve that indicates local

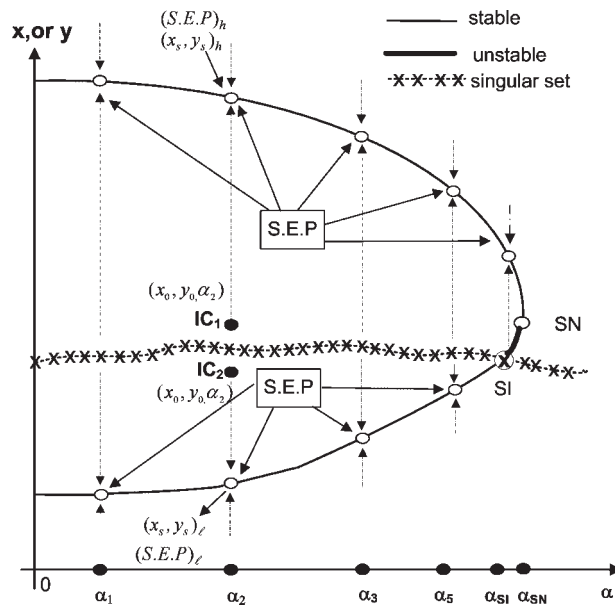


Figure 1. Illustration of equilibrium surface with a singular set, and stability characteristics of the equilibrium points in a nose curve.

bifurcations of the equilibria, and singular points. Note that there are two equilibrium points, namely high voltage (upper) and low voltage (lower) equilibrium points, for any given parameter value until the tip of the nose curve. All equilibrium points located at the upper part of the nose curve are small-signal stable. However, as the bus injections are increased through the bifurcation parameter α , at $\alpha = \alpha_{SI}$ the low voltage equilibrium point undergoes a stability exchange (stable \rightarrow unstable) due to an SI bifurcation and it becomes a type-1 unstable equilibrium point. Further increase in the parameter α causes the high and low voltage equilibria to meet at an SN bifurcation for $\alpha = \alpha_{SN}$. If the parameter α increases beyond the bifurcation value, $\alpha = \alpha_{SN}$ then the system equilibrium disappears and there are no other equilibrium points nearby. The consequence of the loss of equilibria is that the system states change dynamically. In particular, dynamics can be such that the system voltages fall in a voltage collapse.

Figure 1 also illustrates various singular points that are labeled by (x) as the bifurcation parameter α varies. Note that $\alpha = \alpha_{SI}$ the nose curve crosses the singular set, which indicates an SI bifurcation point and a stability exchange. According to the stability characteristics of the equilibrium points, one can draw arrows as shown by dashed lines in Figure 1 to represent trajectories around the equilibrium points. At a given parameter value, say $\alpha = \alpha_2$ both high and low voltage equilibrium points, $(S.E.P)_h$ and $(S.E.P)_l$ are dynamically stable and each one belongs to a different voltage causal region. Note that two distinct trajectories shown by dashed line emanate from the singular point $\alpha = \alpha_2$ and reach high and low voltage stable equilibrium points labeled as $(x_s, y_s)_h$ and $(x_s, y_s)_l$. Such a singular point can be viewed as a source since trajectories come out from this singular point. In response to a temporary disturbance such as a step increase in load or generation, the system state might be located around the singular points after the disturbance is removed. The location of the initial point for the system trajectory with respect to the singular points determines to which of these equilibrium points trajectory

will eventually converge. In Figure 1, two initial points, IC_1 and IC_2 , which are arbitrarily close to the singular point at $\alpha = \alpha_2$ are shown. It is expected that the trajectory starting at the initial point IC_1 above the singular point will converge to the high voltage equilibrium point $(x_s, y_s)_h$ while the other one initiated at the point IC_2 below the singular point will converge to the low voltage equilibrium point $(x_s, y_s)_\ell$. However, this equilibrium point, though stable, is not a feasible operating point due to its low voltage profiles, which may cause a further disturbance in the system leading to a short-term voltage collapse problem. The singular point at $\alpha = \alpha_2$ or at any other parameter value lies on the boundary of the stability region of the corresponding equilibrium point and it qualitatively affects the dynamic behavior of the DAE power system model. Thus, singular points constitute important organizing elements of power system DAE model and needs to be taken into account for the identification of the stability boundaries of an operating point.

In the following section, simulation results for a 5-bus power system are given to illustrate the bifurcations of equilibria, decomposition of constraint manifold into voltage causal regions and singular points, and qualitative effects of singular points on the voltage dynamics of the system.

3. POWER SYSTEM APPLICATION

In this section, we study the bifurcation and algebraic singularities of a 5-bus power system and investigate the structure of constraint manifold (i.e., the union of voltage casual regions and singular points) to analyze the system dynamics and voltage stability issues in the presence of algebraic singularities. Voltage Stability Toolbox (VST) [20] has been used to determine the bifurcation diagrams (nose curves), singular points and to perform time-domain simulations. VST is Matlab-based [21] software package developed by the author to investigate bifurcation and voltage stability issues in power systems. The 5-bus power system, whose one-line diagram is shown in Figure 2, has three generators ($n_g = 3$) and two constant PQ load buses ($n_{pq} = 2$) [4]. Therefore, the DAE model of this 5-bus power system consists of four differential and four algebraic equations. The base case bus injections in per unit (pu) with a 100MW base are as follows: $P_g^0 = [P_2 \ P_3]^T = [5 \ 5]^T$; $P_\ell^0 = [P_4 P_5]^T = [-10 \ -5]^T$; and $Q_\ell^0 = [Q_4 \ Q_5]^T = [-3 \ -2]^T$ pu. Generators, which are uniformly damped ($D = 0.25$) with unity inertia, have the internal voltages $E = [1.2 \ 1.2 \ 1.2]^T$ pu that are

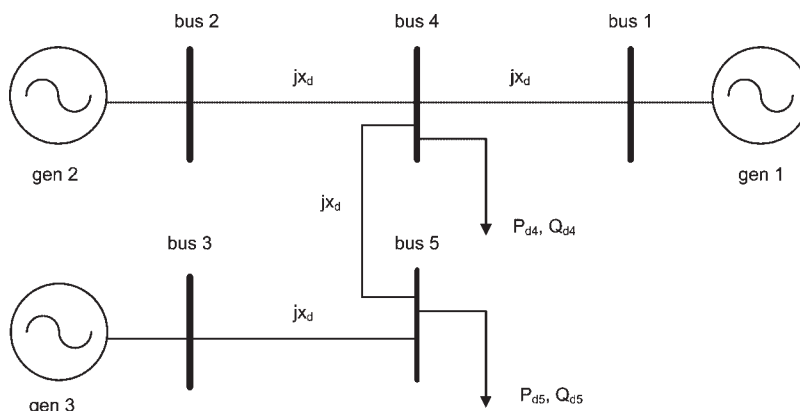


Figure 2. One-line diagram of the 5-bus electric power system.

equal to terminal voltages since the reactance $x_d = 0.1$ pu includes the transient reactances of the generator and transmission line. The generator 1 is chosen as the swing bus with zero angle and all the other phase angles are measured relative to the swing bus.

3.1. Local bifurcations and voltage causal regions

In order to determine a set of equilibrium points, we vary power injections into the generators bus #2 and #3 (P_2 and P_3); and real/reactive power demand at bus 4 while the power factor is kept constant at this bus. The resulting search direction in the bus injection space is as follows: $d_{P_g}^0 = [0.5 \ 0.5]^T$; $d_{P_\ell}^0 = [-0.5 \ 0]^T$; $d_{Q_\ell}^0 = [-0.15 \ 0]^T$. Figure 3 illustrates how the equilibria for the voltage magnitude at bus 4 (U_4) and their corresponding stability characteristics change with parameter variations. Observe that as the parameter α varies, the system equilibria undergo SI and SN bifurcations labeled as SI (S_1) and SN. As the bus injections are increased through the scalar parameter α both high voltage equilibrium ($S.E.P)_h$ and low voltage equilibrium ($S.E.P)_\ell$ are dynamically stable. However, at $\alpha_{SI} = 0.785$ low voltage equilibrium point undergoes a stability exchange (stable \rightarrow unstable) due to an SI bifurcation and it becomes a type-1 unstable equilibrium point. Further increase in the parameter α causes the high and low voltage equilibria to meet at an SN bifurcation for $\alpha_{SN} = 0.8$. The small-signal stability properties of equilibria, and SN and SI bifurcations are determined by monitoring the eigenvalues of system matrix given by Equation (3) as the system moves from one equilibrium point to another along the nose curve with changes in the bifurcation parameter α . A detailed analysis of the evolution of the system matrix eigenvalues could be found in Reference [13].

Figure 3 also shows singular points at various values of α along the nose curve, which are depicted by (x) and labeled as S_1 . It is worth mentioning here that there are multiple singular points at any given parameter α . However, we are interested in those that eventually meet with one of the equilibria located in the lower branch of the nose curve as the parameter α is subject to vary as illustrated in Figure 3. Note that the singular point S_1 at $\alpha_{SI} = 0.785$ coincides with low voltage equilibrium indicating a SI bifurcation. In Figure 3, we also depict another singular point (S_2) for $\alpha = 0.4$ and $\alpha_{SI} = 0.785$ as to

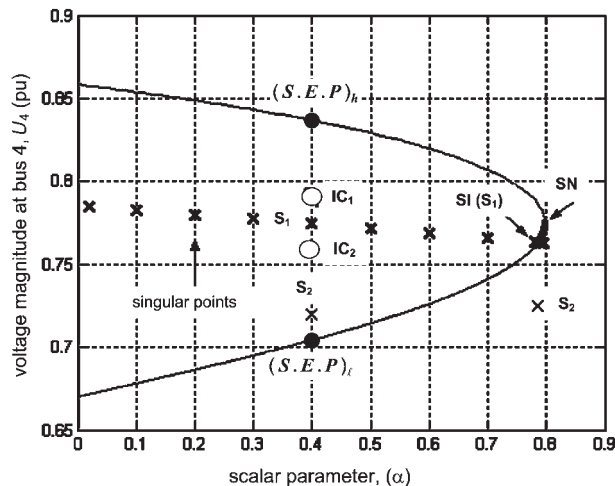


Figure 3. Voltage magnitude at bus 4 (U_4) and singular points vs. parameter alpha (α).

clearly show the relative locations of other singular points that are not associated with the SI bifurcation.

The relative location of singular points with respect to equilibria and SI bifurcation point can be clearly seen using 2-D projections of the constraint manifold. Figure 4(a) shows such a projection of the constraint manifold onto the (δ_2, U_4) -space for $\alpha = 0.4$. The constraint manifold consists of two voltage causal regions (C_0 and C_1) separated by singular points S_1 and S_2 . Note that each region contains a stable equilibrium point labeled as $(S.E.P)_h$ and $(S.E.P)_\ell$. These equilibrium points correspond to the high and low voltage equilibrium points at $\alpha = 0.4$ shown in Figure 3. Singular points S_1 and S_2 are the same as shown in Figure 3 at $\alpha = 0.4$. It will be informative to illustrate the occurrence of the SI bifurcation by using the constraint manifold projection. Figure 4(b) shows the same 2-D projection onto the (δ_2, U_4) -space for $\alpha_{SI} = 0.785$. This time, however, the low voltage equilibrium point $(S.E.P)_\ell$ moves along the region C_1 as α increases from $\alpha = 0.4$ to $\alpha_{SI} = 0.785$ and coincides with the singular point S_1 while the high voltage one, $(S.E.P)_h$, stays in the region C_0 . Note that for this load increase pattern, both equilibria move toward the singular point S_1 not toward S_2 along the regions as the parameter α varies. Therefore, S_2 or any other singular points rather than S_1 are not associated with the SI bifurcation. It must be noted that unstable equilibrium points (UEPs) do not exist within a particular voltage causal region. In such a case, stability boundary is completely determined by singular points.

3.2. Voltage stability analysis

In order to analyze voltage dynamics of the DAE power system model in the presence of algebraic singularities, two initial conditions that are arbitrarily close to the singular point S_1 are selected and time-domain simulations are carried out at $\alpha = 0.4$. The numerical values of initial conditions (IC_1 and IC_2), singular point (S_1) and two equilibrium points ($(S.E.P)_h$ and $(S.E.P)_\ell$) are given in Table I. Moreover, for the algebraic state U_4 these points are also depicted in the nose curve given in Figure 3.

By superimposing the time-domain simulations on the constraint manifold, one could easily visualize the evolution of trajectories in each voltage region and the relative location of initial points with respect to the singular point. Figure 5(a) and (b) show two distinct trajectories initiated at points IC_1 and IC_2 around the singular point S_1 in the (δ_3, U_4) -space and (δ_3, U_5) -space for $\alpha = 0.4$, respectively. Note that Figure 5 illustrates only the related segment of the constraint manifold and voltage causal regions that include two stable equilibrium points and a singular point S_1 . Trajectories

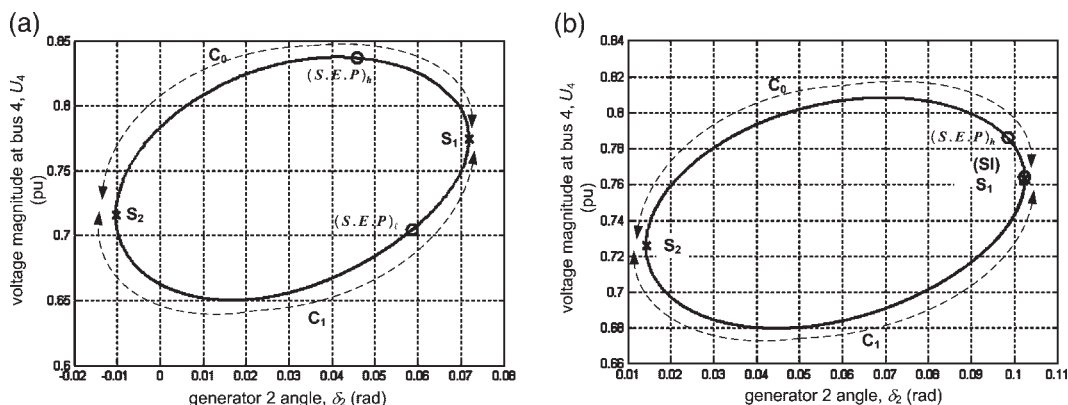


Figure 4. Constraint manifold projections onto the (δ_2, U_4) -space (a) $\alpha = 0.4$ (b) $\alpha = 0.785$.

Table I. Summary of states and initial conditions at $\alpha = 0.4$.

States	δ_2 (rad)	δ_3 (rad)	U_4 (pu)	δ_4 (rad)	U_5 (pu)	δ_5 (rad)
IC ₁	0.07030	0.33308	0.79622	-0.49254	0.70455	-0.38831
IC ₂	0.07038	0.33376	0.75177	-0.53612	0.64751	-0.44358
S ₁	0.07194	0.34821	0.77475	-0.51064	0.67386	-0.40677
(S.E.P) _h	0.04595	0.10748	0.83675	-0.49843	0.79575	-0.46838
(S.E.P) _l	0.05863	0.22498	0.70432	-0.60403	0.61436	-0.55786

initiated at the point IC₁ and labeled by squares remain in the voltage causal region C₀ and reach the high voltage equilibrium point (S.E.P)_h located at this region at $t = 40$ s. Similarly, trajectories started at the point IC₂ and labeled by diamonds remain in the other voltage causal region C₁ and converge to the low voltage equilibrium point (S.E.P)_l. It must be noted that two initial conditions could be considered as the same point quantitatively, especially for the phase angles (see Table I), and their location is very close to the singular point S₁. However, as Figure 5 illustrates, each lies in a different voltage region and more importantly, results in two qualitatively distinct dynamic behaviors of the system.

The evolution of trajectories in time for the two initial conditions given (Table I) is presented in Figure 6 for generator 3 angle (δ_3), and voltage magnitudes of bus 4 and 5 (U_4 , U_5). Note that these simulation results for δ_3 , U_4 , and U_5 were projected onto the corresponding constraint manifolds and previously shown in Figure 5. In Figure 6, the solid-line trajectories are those that start at the point IC₁ and evolve in the voltage causal region C₀ as shown in Figure 5 by squares while the dashed-line trajectories correspond to those that initiate at the point IC₂ and evolve in the other region C₁ as depicted in Figure 5 by diamonds. These simulation results clearly validate the small-signal stability features of the high and low voltage equilibrium points, (S.E.P)_h and (S.E.P)_l, which were previously determined as stable by checking the eigenvalues of the reduced system matrix. As can be seen from Table I, the phase angle deviations between the two stable equilibrium points are not significant, and

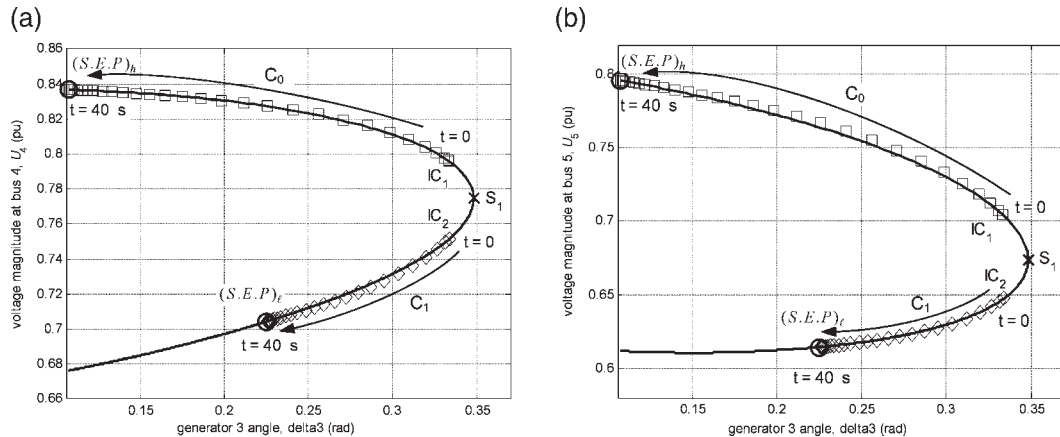


Figure 5. Evolution of trajectories on the constraint manifold for initial conditions around the singular point S₁ for $\alpha = 0.4$ (a) δ_3 vs. U_4 (b) δ_3 vs. U_5 .

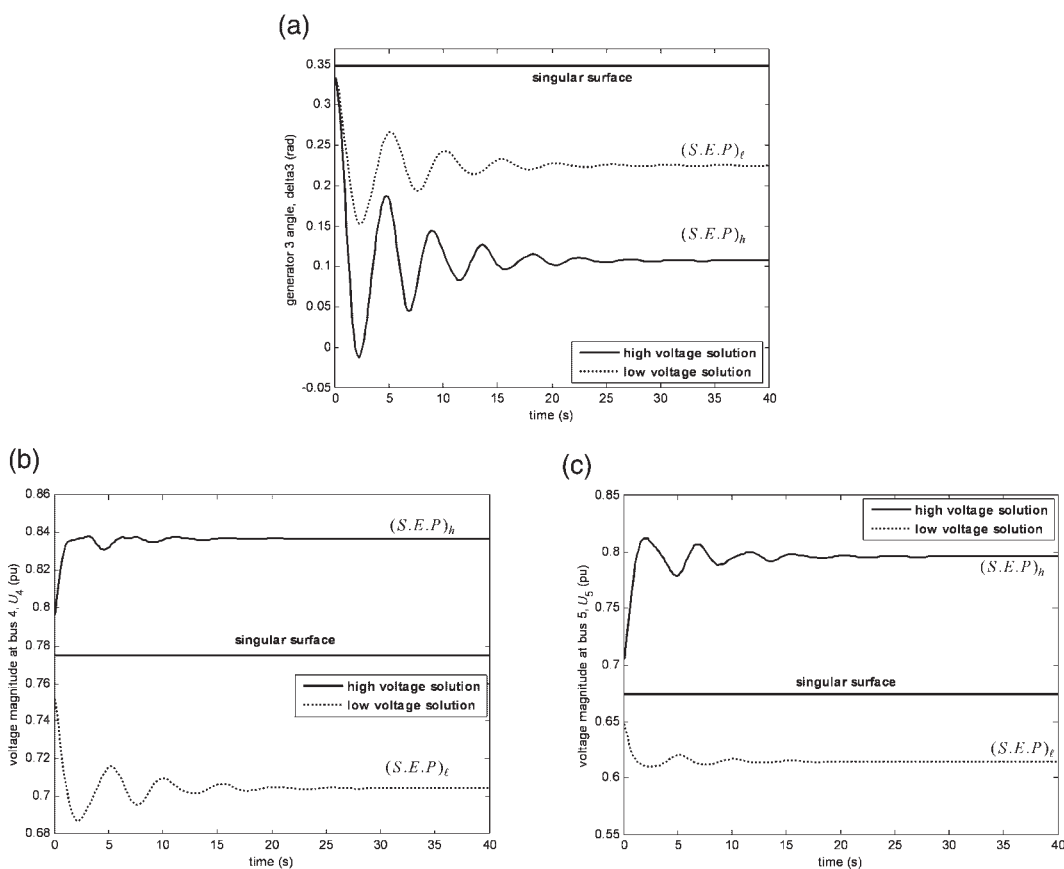


Figure 6. Evolution of system trajectories initiated in two different voltage causal regions (a) generator 3 angle, δ_3 (b) voltage magnitude at bus 4, U_4 (c) voltage magnitude at bus 5, U_5 .

thus angular stability is not a major concern in the presence of algebraic singularities. For example, Table I shows that $\delta_3 = 0.10748$ rad at the equilibrium point $(S.E.P)_h$ and $\delta_3 = 0.22498$ at $(S.E.P)_l$. On the other hand, as Figure 5 shows, the location of the singular point on the constraint manifold determines whether the voltage trajectories will eventually settle to $(S.E.P)_h$ or $(S.E.P)_l$. Figure 6(b) and (c) indicate that depending on the location of initial conditions with respect to the singular point, the bus voltages can follow two possible paths each leading to a different stable equilibrium point. Observe that if the system trajectory starts at point above the singular point (the point IC_1 in Figure 5), it will reach to the high voltage equilibrium point $(S.E.P)_h$, which is a normal operating point. If it starts at a point below the singular point (the point IC_2 in Figure 5) it will converge to the low voltage equilibrium point $(S.E.P)_l$, which is not a feasible operating point. For example, from Table I one can see that bus voltage magnitude $U_4 = 0.83675$ pu at the equilibrium point $(S.E.P)_h$ while $U_4 = 0.70432$ pu at $(S.E.P)_l$.

It is possible that the system may try to settle to an infeasible operating point, as in this example. Invariably at least one bus will have low voltage at that point, so overloads are likely. Protection action,

such line tripping or load shedding, will usually occur, disturbing the system further and leading to a short-term voltage collapse.

4. DISCUSSION

Many other researchers [2,5,11,12,14,15] have used constant power model in bifurcation and singularity analysis of DAE power system model. However, a more accurate load model that faithfully reflects the nonlinear dynamical behavior of the physical load components should be included in the DAE model in order to obtain more physically relevant results since load models have significant impact on voltage stability of power systems [22,23]. In large-scale transient/voltage stability simulations, loads are typically modeled as static (algebraic) functions of voltage and possibly frequency [24,25].

Moreover, in DAE model, the structure of the constraint manifold of (4) and the existence of the singular surface defined by Equation (8) are closely related to load models. For example, in classical transient stability models, loads are generally assumed to consist of constant admittances. In that case, algebraic (network) equations of DAE model of (1) may be written as linear complex current–voltage relationships. A solution of these equations always exists for an interconnected power network, so algebraic singularity cannot occur. On the other hand, in voltage stability analysis of DAE power system model, the frequency dependency of the load is usually ignored and loads are modeled as the exponent of bus voltage magnitude [17,18]:

$$\begin{aligned} P_{di} &= P_{di}^0 |U_i|^{k_{p_i}} \\ Q_{di} &= Q_{di}^0 |U_i|^{k_{q_i}} \end{aligned} \quad i = 1, 2, 3, \dots, n_g + n_{pq} \quad (12)$$

where P_d^0 and Q_d^0 are real and reactive power operating points, respectively, and k_p and k_q active and reactive power indices or exponents, respectively.

Although the use of such load models is necessary to represent the true nonlinear characteristics of loads in DAE power system model, one must be careful in selecting load indices in order not to lose some essential singularity properties of DAE system. It is reported in the literature that the existence of the singular surface depends on the relationship between the bus voltage and load demand. Specifically, the variation of the load indices used in Equation (12) to model load may cause significant structural changes to the voltage causal region/singular surface decomposition of the constraint manifold [17,18,26]. For certain values of load indices, algebraic singularity may not occur, which implies the global voltage causality. In References [17] and [18], Hiskens proposes a conjecture on conditions which ensure global voltage causality with the load model of (12). For reasonable values of network admittance (i.e., the admittance matrix of the load bus network is negative definite) and signs on P_d^0 and Q_d^0 (i.e., $P_d^0 > 0$ and $Q_d^0 > 0$) the conditions include either

$$k_p \geq 1 \quad \text{when} \quad k_q = 2k_p \geq 1 \quad \text{when} \quad k_p = 2 \quad (13)$$

It was also shown in Reference [17] that this conjecture can be proven for one- or two-bus power system. Effects of variation of the load indices on the voltage causality and algebraic singularity of a two-bus system have been extensively studied and similar voltage dynamics for noncausal load indices have been presented in Reference [18]. In Reference [26], similar conditions ($Q_d^0 > 0, k_p, k_q > 1$) have been proposed and proven for any size of power systems. It must be noted that these conditions that guarantee the global voltage causality are not always satisfied in practice [25,27] (see Table 3.1 in page

530 of Reference [25] for range of active and reactive power load indices for residential, commercial, and industrial loads). Therefore, algebraic singularity and its qualitative effects on the voltage dynamics are still important matters in the DAE power system model when the voltage-dependent load model is used in the analysis.

5. CONCLUSIONS

This paper has investigated local bifurcations and algebraic singularities of DAE power system model for the voltage stability assessment using small-signal stability analysis and time-domain simulations. When the system load is increased, the occurrence of SI and SN bifurcation has been observed. The SI bifurcation, unlike the SN bifurcation, is typical of DAE power system model rather than ODE model.

Algebraic singular points have been determined at various load levels and depicted in the nose curve together with the equilibria. It has been found that the location of singular points smoothly varies as the load demand increases from its nominal value to the maximum loading point (the SN bifurcation point). The depiction of singular points together with the equilibria and their corresponding local bifurcations as a function of the system load provides a comprehensive picture of the stability of the DAE model. Moreover, to use DAE as a tool for the analysis of power system dynamics, knowledge of where singular points are located and how their location are changed with respect to parameters can be applied toward the definition of “limits” of appropriateness for a given model. The relative location of singular points with respect to equilibria and the occurrence of SI bifurcation have been clearly shown using 2-D projections of the constraint manifold.

The investigation of the structure of the constraint manifold has resulted that the constraint manifold consists of voltage causal regions surrounding a stable equilibrium point and singular points connecting them. More importantly, it is further shown that UEPs may not exist in a particular region and thus, the singular points strictly define the boundary of the region of attraction (stability region) of stable equilibria. Time-domain simulations indicate that depending on the location of initial points, each of which are located in a different voltage region and arbitrarily close to a singular point, the trajectories of bus voltage magnitudes can follow different paths each leading to the stable equilibrium point in that region. However, some of these equilibrium points may not be a feasible operating point due to their low voltage profiles, which may cause a further disturbance in the system leading a voltage stability problem.

Future work will be focused on integrating realistic static and dynamic load models into the DAE model. Voltage Stability Toolbox (VST) [20] used for simulation is now being updated to include more realistic load models and in the near future we will be able to investigate the qualitative effects of load indices on the decomposition of the constraint manifold and singularity of the algebraic equation for larger power system.

6. LIST OF SYMBOLS AND ABBREVIATIONS

$x \in \mathcal{R}^n$	vector of dynamic state variables such as generator angles and velocities
$y \in \mathcal{R}^m$	vector of algebraic state variables such as load bus voltage magnitudes and phase angles
$\beta \in \mathcal{R}^k$	vector of parameters such as loads
$f(\bullet)$	swing equation describing dynamics of each generator
$g(\bullet)$	power flow equations representing real and reactive power balances at the load buses

E	set of equilibrium points
A_{sys}	reduced (linearized) system matrix
D_y	Jacobian matrix with respect to variable y
M	principal component of the constraint manifold
C_p	voltage causal region or solution sheet
p	voltage causal region index
$S(\beta)$	set of singular points
$SI(\beta)$	set of singularity-induced bifurcation points
P_g	net real power injections to the $n_g - 1$ number of generators
β_ℓ	load demands at the n_{pq} number of load buses
P_ℓ	real power demand
Q_ℓ	reactive power demand
β^0	base case bus injections
α	scalar bifurcation parameter
direction β	direction vector in the parameter space
$(x_s, y_s)_h$	high voltage stable equilibrium point
$(x_s, y_s)_\ell$	low voltage stable equilibrium point
c	scalar parameter
δ	phase angle
U	voltage magnitude
DAE	differential-algebraic equation
SN	saddle node
SI	singularity induced
$(S.E.P)_h$	high voltage stable equilibrium point
$(S.E.P)_\ell$	low voltage stable equilibrium point
IC	initial condition

REFERENCES

1. Kilani KB, Schlueter RA. Trends in model development for stability studies in power system. *Electric Power System Research* 2000; **53**:207–215.
2. Kwatny HG, Pasrija AK, Bahar LY. Static bifurcations in electric power networks: loss of steady state stability and voltage collapse. *IEEE Transactions on Circuits and Systems* 1986; **33**:981–991.
3. Venkatasubramanian V, Schättler H, Zaborszky J. Global voltage dynamics: study of a generator with voltage control, transmission and matched MW load. *IEEE Transactions on Automatic Control* 1992; **37**:1717–1733.
4. Praprost KL, Loparo KA. An energy function method for determining voltage collapse during a power system transient. *IEEE Transactions on Circuits and Systems* 1994; **41**:635–651.
5. Lee B, Ajarapu V. A piecewise global small-disturbance voltage-stability analysis of structure-preserving power system models. *IEEE Transactions on Power Systems* 1995; **10**:1963–1971.
6. Kim K, Schättler H, Venkatasubramanian V, Zaborszky J, Hirsch P. Methods for calculating oscillations in large power systems. *IEEE Transactions on Power Systems* 1997; **12**:1639–1648.
7. Zhou Y, Ajarapu V. A fast algorithm for identification and tracing of voltage and oscillatory stability margin boundaries. *Proceedings of IEEE* 2005; **93**:934–946.
8. Gou T, Schlueter RA. Identification of generic bifurcation and stability problems in power system differential-algebraic model. *IEEE Transactions on Power Systems* 1994; **9**:1032–1044.
9. Kwatny HG, Fischl R, Nwankpa CO. Local bifurcation in power systems: theory, computation, and application. *Proceedings of IEEE* 1995; **83**:1456–1483.

10. Venkatasubramanian V, Schättler H, Zaborszky J. Local bifurcations and feasibility regions in differential-algebraic systems. *IEEE Transactions on Automatic Control* 1995; **40**:1992–2013.
11. Makarov YV, Hill DJ, Dong ZY. Computation of bifurcation boundaries for power systems: a new Δ -plane method. *IEEE Transactions on Circuits and Systems* 2000; **47**:536–544.
12. Lerm AP, Canizares CA, Silva AS. Multi-parameter bifurcation analysis of the South Brazilian power system. *IEEE Transactions on Power Systems* 2003; **18**:737–746.
13. Ayasun S, Nwankpa CO, Kwatny HG. Computation of singular and singularity induced bifurcation points of differential-algebraic power system model. *IEEE Transactions on Circuits and Systems* 2004; **51**:1525–1538.
14. Marszalek W, Trzaska ZW. Singularity-induced bifurcations in electrical power systems. *IEEE Transactions on Power Systems* 2005; **20**:312–320.
15. Guoyun C, Hill DJ, Hui R. Continuation of local bifurcations for power system differential-algebraic equation stability model. *IEEE Proceedings on Generation Transmission and Distribution* 2005; **152**:575–580.
16. DeMarco CL, Bergen AR. Applications of singular perturbation techniques to power system transient stability analysis. *IEEE International Symposium on Circuits and Systems, Proceedings*, 1984; 597–601.
17. Hiskens IA, Hill DJ. Energy function, transient stability and voltage behavior in power systems with nonlinear loads. *IEEE Transactions on Power Systems* 1989; **4**:1525–1533.
18. Hiskens IA, Hill DJ. Failure modes of a collapsing power system. *Bulk Power System Voltage Phenomena II—Voltage Stability and Security*, Deep Creek Lake, Maryland, *Proceedings*, 1991, pp. 53–63.
19. Ayasun S, Nwankpa CO, Kwatny HG. An efficient method to compute singularity induced bifurcations of decoupled parameter-dependent differential-algebraic power system model. *Applied Mathematics and Computation* 2005; **167**:435–453.
20. Ayasun S, Nwankpa CO, Kwatny HG. Voltage stability toolbox for power system education and research. *IEEE Transactions on Education* 2006; **49**:432–442.
21. MATLAB. *High-performance numeric computation and visualization software*. The Mathworks Inc.: Natick, MA, 2001.
22. Taylor C. *Power System Voltage Stability*. Power System Engineering. McGraw-Hill: New York, 1994.
23. Hill D. Nonlinear dynamic load models with recovery for voltage stability studies. *IEEE Transactions on Power Systems* 1993; **8**:166–176.
24. IEEE Task Force on Load Representation for Dynamic Performance (Contributors: Price WW, Taylor CW, Rogers GJ, Sirivasan K, Concordia C, Pal MK, Bess KC, Kundur P, Agrawal BL, Luini JF, Vaahedi E, Johnson BK.). Standard load models for power flow and dynamic performance simulation. *IEEE Transactions on Power Systems* 1995; **10**:1302–1313.
25. IEEE Task Force on Load Representation for Dynamic Performance (Contributors: Price WW, Casper SG, Nwankpa CO, Bradish RW, Chiang HD, Concordia C, Staron JV, Taylor CW, Vaahedi E, Wu G.). Bibliography on load models for power flow and dynamic performance simulation. *IEEE Transactions on Power Systems* 1995; **10**:523–538.
26. Lesieutre BC, Sauer PW, Pai MA. Existence of solutions for the network/load equations in power systems. *IEEE Transactions on Circuits and Systems* 1999; **446**:1003–1011.
27. Concordia C, Ihara S. Load representation in power system stability studies. *IEEE Transactions on Power Apparatus and Systems* 1982; **101**:969–977.

AUTHOR'S BIOGRAPHY



Saffet Ayasun received the B.S. degree in Electrical Engineering from Gazi University, Ankara, Turkey in 1989, M.S. degrees in Electrical Engineering and Mathematics from Drexel University, Philadelphia, PA, in 1997 and 2001, respectively, and Ph.D. in Electrical Engineering from Drexel University in 2001. He is currently working as an Assistant Professor in the Electrical Engineering Department of Nigde University, Turkey. His research interests include modeling and stability analysis of dynamical systems, applied mathematics, nonlinear control theory, bifurcation theory and its application into power systems stability analysis.